

G	G	T	C	8	3	5	Operator: Ling yan	b	Dispatch: 05.01.20	PE: Asdis Thorsteinsson
	Journal Name			Manuscript No.			Proofreader: Liu MaoJuan		No. of Pages: 8	Copy-editor: Christine Sanders

53BP2 induces apoptosis through the mitochondrial death pathway

Shinya Kobayashi^{1,2,*}, Shinichi Kajino^{1,2,*}, Naoko Takahashi¹, Satoshi Kanazawa¹, Kenichi Imai¹, Yurina Hibi¹, Hirotaka Ohara², Makoto Itoh² and Takashi Okamoto^{1,*}

¹Department of Molecular and Cellular Biology, Nagoya City University Graduate School of Medical Sciences, 1 Kawasumi, Mizuho-cho, Mizuho-ku, Nagoya, Aichi 467-8601, Japan

²Department of Internal Medicine and Bioregulation, Nagoya City University Graduate School of Medical Sciences, 1 Kawasumi, Mizuho-cho, Mizuho-ku, Nagoya, Aichi 467-8601, Japan

The p53 binding protein 2 (53BP2) has been identified as the interacting protein to p53, Bcl-2, and p65 subunit of nuclear factor κ B (NF- κ B). The TP53BP2 gene encodes two splicing variants, 53BP2S and 53BP2L, previously known as apoptosis stimulating protein 2 of p53 (ASPP2). We found that these 53BP2 proteins are located predominantly in the cytoplasm and induce apoptosis as demonstrated by cleavage of poly ADP ribose polymerase (PARP) and annexin V staining. Furthermore, we demonstrate that 53BP2 is located in the mitochondria and induces apoptosis associated with depression of the mitochondrial trans-membrane potential ($\Delta\Psi_m$) and activation of caspase-9. From these findings we conclude that 53BP2 induces apoptosis through the mitochondrial death pathway.

Introduction

Apoptosis is a well-defined biochemical pathway and is essential for the maintenance of cellular homeostasis in metazoans. Accumulating evidences indicate that the normal apoptotic pathway is affected in the pathological processes such as cancer and autoimmunity (Fisher *et al.* 1995; Green & Reed 1998; Jackson & Puck 1999; Daniel & Korsmeyer 2004). The induction of apoptosis occurs through two distinct pathways, the one elicited by death receptors in the plasma membrane ('extrinsic pathway') and the other directly involving mitochondria ('intrinsic pathway'). Whereas the former primarily involves activation of caspase-8, the latter apoptosis pathway is associated with the release of cytochrome C from mitochondria and activation of caspase-9 (for a review see Judith *et al.* 2004).

The p53 binding protein 2 (53BP2) has been initially identified as an interacting protein to p53 (Iwabuchi *et al.* 1994) and implicated in the biological action of p53. It was also shown that the 53BP2 binding site in the p53 core domain is evolutionarily conserved and

is frequently mutated in human cancer (Iwabuchi *et al.* 1994; Gorina & Pavletich 1996). The subsequent studies have revealed that it interacts with Bcl-2 (Naumovski & Cleary 1996), and p65 subunit of nuclear factor κ B (NF- κ B) (Yang *et al.* 1999). Interestingly, 53BP2 has been shown to induce apoptosis (Yang *et al.* 1999), which was confirmed by others (Lopez *et al.* 2000; Ao *et al.* 2001; Samuels-Lev *et al.* 2001; Bergamaschi *et al.* 2004). However, the mechanism by which 53BP2 induces apoptosis has not been clarified.

53BP2 protein is encoded by a single copy gene TP53BP2 located in the long arm of chromosome 1 at q42.1 (Yang *et al.* 1997). We have recently found that it encodes two distinct mRNA species, either with or without exon 3, by alternative splicing (Takahashi *et al.* 2004) (Fig. 1A). These splicing variants encode two 53BP2 proteins containing 1005 and 1128 amino acids (aa) with the longer isoform containing additional 123 amino acids in the N-terminus where no known functional motif or distinct intracellular localization signal is found. Although Samuels-Lev *et al.* (2001) renamed the longer 53BP2 isoform as ASPP2 (apoptosis stimulating protein of p53 2), we have proposed to call these proteins as 53BP2S (short) and 53BP2L (long) based on the genome organization of TP53BP2 transcripts (Takahashi *et al.* 2004). 53BP2 proteins contain several structural and functional

Communicated by: Masayuki M. Yamamoto

*Correspondence: E-mail: tokamoto@med.nagoya-cu.ac.jp

*These two authors contributed equally to this work.

DOI: 10.1111/j.1365-2443.2005.00835.x

© Blackwell Publishing Limited

Genes to Cells (2005) 10, 000–000 1

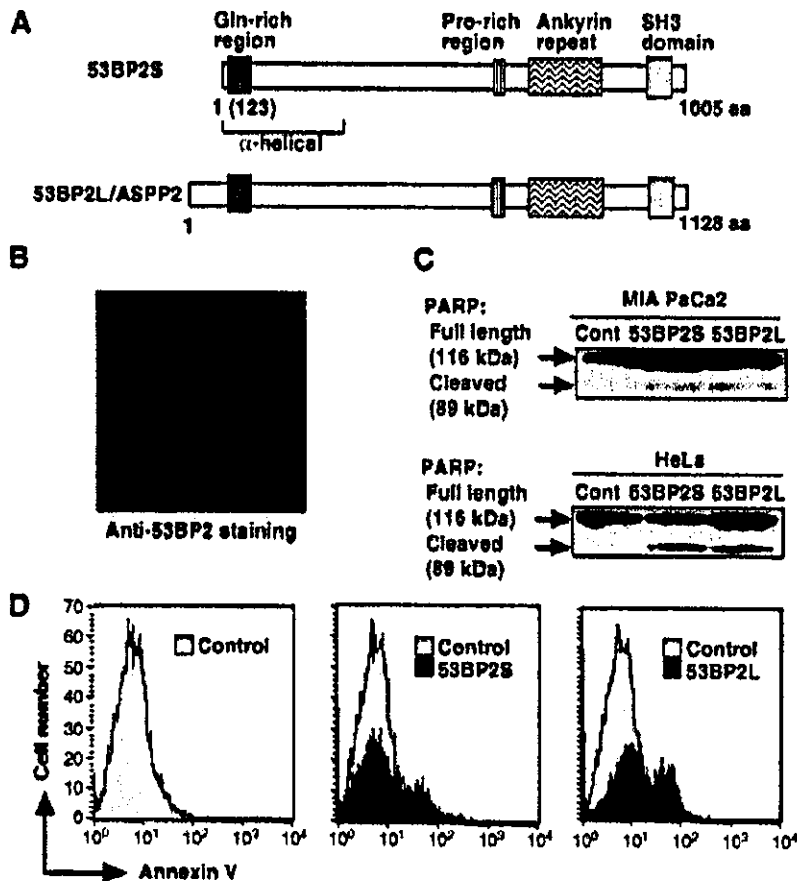


Figure 1 Induction of apoptosis by 53BP2 proteins. (A) Diagrammatic representation of 53BP2S and 53BP2L/ASPP2 proteins. Locations of Gln-rich region, putative 'α-helical region', Pro-rich region, ankyrin repeats, and SH3 domain are indicated. Two splicing variants, 53BP2S and 53BP2L/ASPP2, containing 1005 amino acids and 1128 amino acids residues, respectively, are encoded by the same gene *TP53BP2* (Takahashi *et al.* 2004). 53BP2L contains additional 123 amino acids N-terminal region containing no apparent functional/structural motifs. (B) The localization of endogenous 53BP2 proteins in MIA PaCa-2 cells. Subcellular localization of endogenous 53BP2 was examined by immunostaining with anti-53BP2 mouse monoclonal antibody. The dim staining of 53BP2 proteins was repeatedly observed, which is presumably due to the low protein stability as previously indicated (Yang *et al.* 1999; Lopez *et al.* 2000). (C) Cleavage of PARP by 53BP2 proteins. MIA PaCa-2 cells and HeLa cells were transfected with pcDNA3.1-53BP2 ('53BP2S') or pCEP4-ASPP2 ('53BP2L') plasmids and the cell lysates were immunoblotted with anti-PARP antibody. The intact form of PARP (116 kDa) and its cleavage form (89 kDa) were detected by an anti-PARP rabbit polyclonal antibody (indicated by arrows). Note that no significant difference of the amounts of the cleaved form of PARP was found in cells expressing 53BP2S and 53BP2L. Cont, cells transfected with a control expression vector pcDNA3.1. (D) Induction of apoptosis by over-expression of 53BP2 proteins. MIA PaCa-2 cells were transfected with pcDNA3.1-53BP2 or pCEP4-ASPP2 and cells undergoing apoptosis were detected by flow cytometry. Live and dead cells were discriminated on the basis of their forward and side light-scattering properties. In order to evaluate cells undergoing apoptosis, cells were stained by both annexin V-PE and 7-AAD and those cells expressing 7-AAD were excluded from the measurement. The transfection efficiency was estimated to be approximately 65% by the GFP expression from the co-transfected pEGFP plasmid. The experiments were repeated more than three times with the same results.

motifs including Gln-rich α-helical region, Pro-rich regions, ankyrin repeats, and Src-homology 3 domain.

In this study, we demonstrate that two 53BP2 isoforms, 53BP2S (previously called '53BP2') and 53BP2L ('ASPP2'), are localized predominantly in the cytoplasm

and similarly induce apoptosis. We found that the mitochondrial death pathway is involved in the 53BP2-mediated apoptosis. The biological roles of 53BP2 and its interacting proteins in the regulation of apoptosis are discussed.

Results

Induction of apoptosis by 53BP2 proteins

Figure 1A illustrates the organization of 53BP2 isoforms as previously reported (Takahashi *et al.* 2004). As shown in Fig. 1B, the endogenous 53BP2 proteins were localized predominantly in the cytoplasm, confirming the previous reports wherein 53BP2 was over-expressed (Iwabuchi *et al.* 1998; Yang *et al.* 1999). To compare the effect of 53BP2S and 53BP2L, these proteins were transduced in MIA PaCa-2 and HeLa cells. After 48 h of transfection, the cleaved form of poly ADP ribose polymerase (PARP; 89 kDa product), a hallmark of apoptosis, was detected (Fig. 1C). When 53BP2S and 53BP2L were over-expressed in MIA PaCa-2 cells, approximately 16% and 27% of cells were found undergoing early apoptotic process (annexin V (+), 7-AAD (-)), respectively, whereas the percentage of apoptotic cells in the control was only 1.8% (Fig. 1D). The extents of apoptosis were similar to our previous observations using various DNA damaging agents (Mori *et al.* 2000).

Induction of apoptosis in a stable transfectant (293/53BP2)

We then examined the action of 53BP2 using the 293/53BP2 cells, in which expression of 53BP2S is under stringent control by ponasteron A (pon A). In Fig. 2A, both 293/53BP2 and its control 293/LZ were treated with pon A. The 53BP2S protein became detectable after 12 h of induction by pon A (5 μ M) in a time-dependent manner and induced apoptosis as early as 24 h after pon A treatment. As shown in Fig. 2B, after 72 h of 53BP2S expression, a significant number (26%) of cells underwent apoptosis as revealed by positive staining for annexin V, whereas only the background level (6.5%) was stained in control cells. Cells at early apoptotic process (annexin V (+), 7-AAD (-)) were found 14% and 3% in 293/53BP2 cells and control cells, respectively (Fig. 2B). No cleavage of PARP or a significant annexin V staining was detected with the control 293/LZ cells (data not shown).

Cytosolic and mitochondrial localization of 53BP2S

In Fig. 3A, intracellular localization of 53BP2S was examined by transfection of pEGFP53BP2 expressing 53BP2S in fusion with green fluorescence protein (GFP). A punctate vesicular pattern was noted, localized predominantly in the cytoplasm of the transfected cells. To confirm the localization of 53BP2S, we co-transfected pDsRed2-Mito, expressing red fluorescent protein targeted to mitochondria. As demonstrated in Fig. 3A and

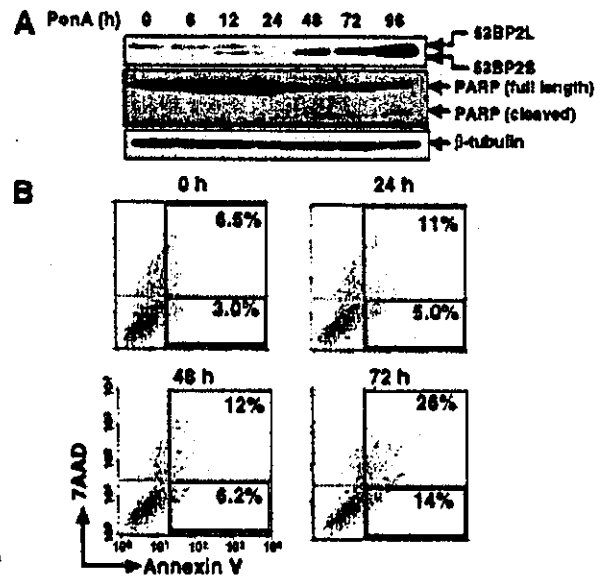


Figure 2 Induction of apoptosis in 293/53BP2 cell line. (A) Time course of induction of 53BP2S and cleavage of PARP in 293/53BP2 cells. Cells were treated with pon A (5 μ M) using an ecdysone-inducible expression system for the indicated periods (h) and the cell lysate (10 μ g protein) was examined for the expression of 53BP2S and PARP. The intact full-length PARP (116 kDa) was cleaved into 89 kDa during the apoptotic process. Longer exposure of chemiluminescence for protein detection revealed the endogenous 53BP2L protein in these cells. β -tubulin was used as an internal control. (B) Flow cytometric detection of apoptotic cells. 293/53BP2 cells were stimulated with pon A (5 μ M) and cultured for the indicated periods (h). The percentages of cells at apoptosis (annexin V (+)) and cells at early apoptosis (annexin V positive and 7-AAD (-)) were counted and indicated separately.

53(B)P2S was shown to be partly localized in the mitochondria in addition to the cytoplasm. In most cells only portions of mitochondria were costained with 53BP2S, suggesting that small amounts of 53BP2S molecules could be sufficient to induce apoptosis. In Fig. 3B, subcellular fractionation was performed and the presence of 53BP2S was examined. Protein expression was induced by pon A for 48 h and each subcellular fraction was subjected to Western blotting with anti-53BP2 antibody. Although majority of the 53BP2S protein was detected in the cytosolic fraction, it was also detected in the mitochondrial fraction (Fig. 3B).

Depression of $\Delta\Psi_m$ by 53BP2S expression

These findings suggested the involvement of the 'intrinsic' death pathway. We thus examined the change in $\Delta\Psi_m$

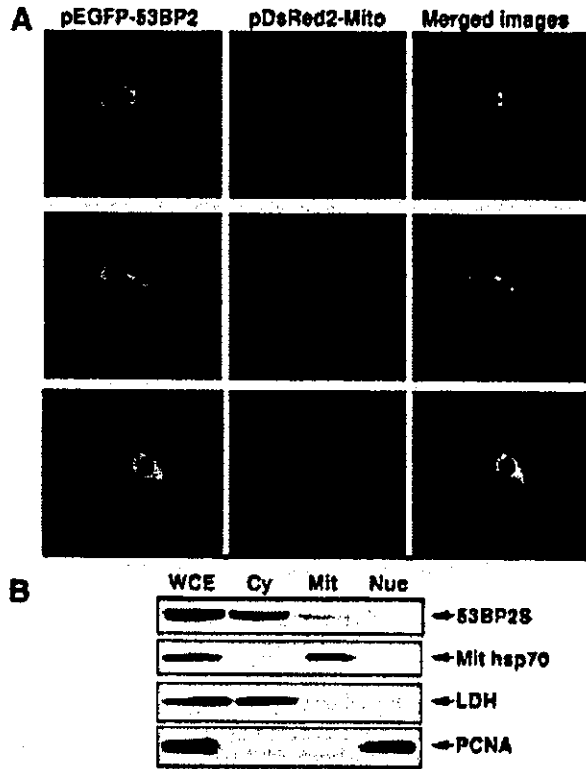


Figure 3 Intracellular localization of 53BP2S. (A) Co-localization of 53BP2S and mitochondria marker. 293 cells were transiently transfected with pEGFP-53BP2 and mitochondria-targeting plasmid pDsRed2-Mit and examined under confocal microscope. The GFP fluorescence, DsRed fluorescence and merged images of cells are shown. Note that only portions of mitochondria (visualized by DsRed) were costained with GFP (53BP2S). (B) Subcellular fractionation. Upon induction of 53BP2 by pon A (5 μ M, 48 h) in 293/53BP2 cells, whole cell extract (WCE) was prepared. The cytoplasmic (Cy), mitochondrial (Mit) and nuclear (Nuc) fractions were separated as described in *Experimental procedures*. Each protein fraction was separated by 10% SDS-PAGE, and probed with antibodies to 53BP2S, PCNA (nuclear marker), mitochondrial heat shock protein (Mit hsp70) and LDH (cytoplasmic marker). The same cell equivalents were loaded on each lane. Contamination of the cytoplasmic fraction into the mitochondria fraction was considered negligible because of the absence of LDH. The identical results were obtained repeatedly.

following 53BP2S expression (Fig. 4). Several cationic, lipophilic, fluorescent dyes such as CMXRos and rhodamine 123, can readily detect changes in $\Delta\Psi_m$ as they are selectively sequestered by respiring mitochondria by virtue of their negative charges on the inner membrane and are washed out when $\Delta\Psi_m$ is lost. As shown in Fig. 4A, the extent of CMXRos staining in pEGFP53BP2-transfected cells (visualized by the expression of GFP)

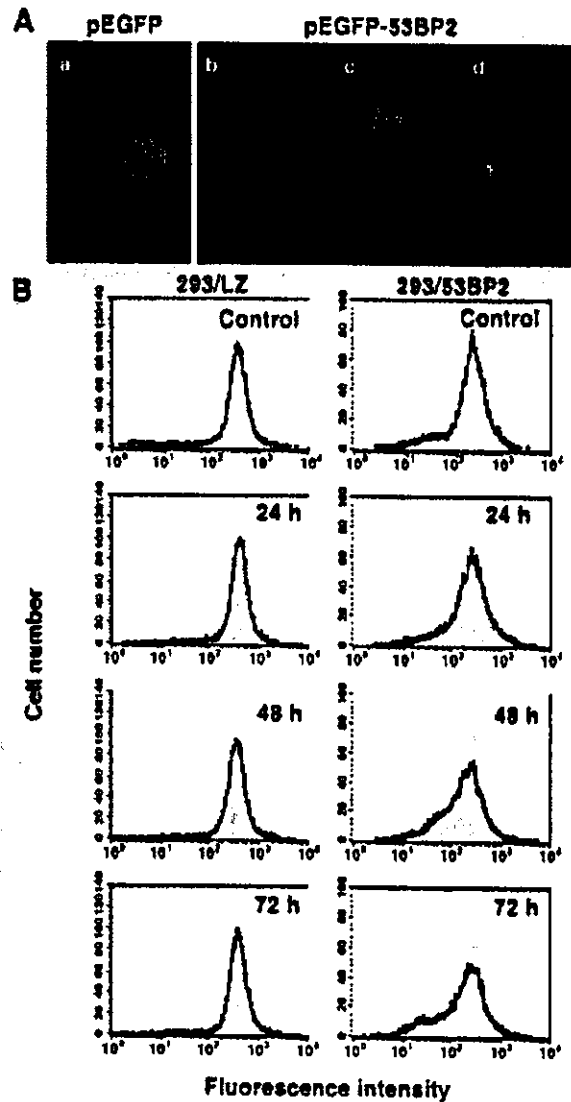


Figure 4 Alteration of the mitochondria transmembrane potential ($\Delta\Psi_m$) by 53BP2S. (A) Reduction of $\Delta\Psi_m$ by 53BP2S. After 48 h of transfection with pEGFP (a) or pEGFP53BP2 (b–d) plasmids, MIA PaCa-2 cells were stained with CMXRos. Typical cells are shown. In cells expressing 53BP2S, progressive reduction of $\Delta\Psi_m$ was observed in association with nuclear fragmentation (from b–d). The same exposure time was used in each picture. (B) Temporal change of $\Delta\Psi_m$ following 53BP2S induction. 293/53BP2 and 293/LZ cells were treated with pon A for indicated periods (h), stained with rhodamine 123, and flow cytometric analysis was performed. Distribution of fluorescence intensity of cells with sham treatment (only the solvent ethanol was added) is shown in gray shadow. 'Control', uninduced cells.

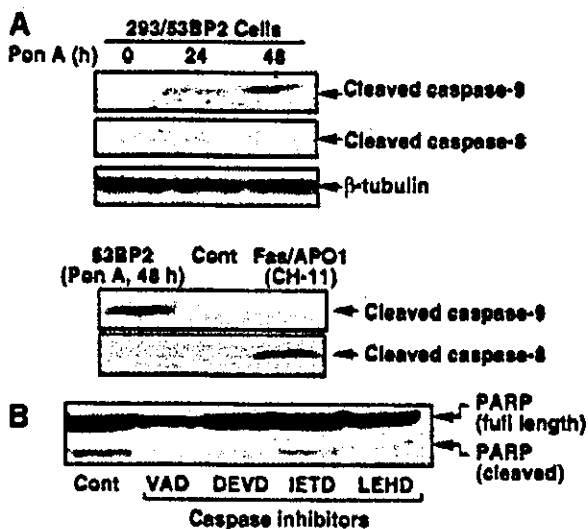


Figure 5 Involvement of caspase-9 in apoptosis induced by 53BP2S. (A) Activation of caspase-9 by 53BP2S. 293/53BP2 cells were treated by pon A (5 μ M) for the indicated periods (h). Each cell lysate (10 μ g protein) was examined for the activated ('cleaved') form of caspase-9 by Western blotting with anti-caspase-9 (cleaved form) or anti-caspase-8 (cleaved form) antibodies (upper panel). β -tubulin was used as an internal control. In the lower panel, 293/53BP2 cells were either stimulated with the agonistic anti-Fas antibody (CH-11) or treated with pon A and the activation of caspase-8 or caspase-9 was similarly examined. (B) Inhibition of the PARP cleavage by caspase inhibitors. 293/53BP2 cells were cultured with or without caspase inhibitors for 12 h and treated with pon A (5 μ M) for 48 h. The cell lysate was prepared and examined for the PARP cleavage by Western blotting. The same amounts of each cell lysate (10 μ g protein) were analyzed. Cont, DMSO alone; VAD, common inhibitor for the caspase-family (Z-VAD-FMK); DEVD, caspase-3-specific inhibitor (Z-DEVD-FMK); IETD, caspase-8-specific inhibitor (Z-IETD-FMK); LEHD, caspase-9-specific inhibitor (Z-IETD-FMK).

was diminished indicating a decrease in $\Delta\Psi_m$. In contrast, no such changes were observed in the control cells transfected with pEGFP. In Fig. 4B, the temporal change of $\Delta\Psi_m$ in 293/53BP2 cells is shown. When 53BP2S was expressed, progressive reduction of $\Delta\Psi_m$ detected by the rhodamine123 fluorescence intensity was observed over time, concomitantly with the appearance of apoptotic cells (compare with Fig. 2B). No such change was observed in control 293/LZ cells.

Involvement of caspase-9 in apoptosis induced by 53BP2S

Finally, to examine the upstream caspase cascade involved in the 53BP2S-mediated apoptosis, 293/53BP2 cell lysates

were prepared after 24 and 48 h of pon A treatment. The presence of activated (cleaved) forms of caspase-8 and caspase-9 were examined in these cells. Figure 5A shows that caspase-9, but not caspase-8, was activated following the induction of 53BP2S. To confirm these observations, the effects of specific inhibitors for caspase-3, -8, and -9 were examined. As shown in Fig. 5B, the effects of peptide inhibitors among all types of known caspases (VAD), caspase-3 (DEVD), caspase-8 (IETD) and caspase-9 (LEHD) were shown. Although VAD, DEVD and LEHD effectively blocked the PARP cleavage induced by 53BP2S, only a minimal effect was observed with IETD. These findings indicate that 53BP2S induces apoptosis through the mitochondrial ('intrinsic') death pathway.

Discussion

The present data have revealed the involvement of mitochondria in the 53BP2-mediated apoptosis. 53BP2 has two protein isoforms, 53BP2S and 53BP2L, generated by alternative splicing (Takahashi *et al.* 2004). These two 53BP2 proteins are localized predominantly in the cytoplasm and exhibited similar biological actions although we do not currently know the reason of such redundancy. In this study, we have explored the proapoptotic action of 53BP2S using transient expression and the stable cell line in which 53BP2 is under the stringent control of pon A. When expressed, 53BP2S was located in the mitochondria and induced cell death associated with $\Delta\Psi_m$ repression, caspase-9 activation, PARP cleavage, annexin V staining, and typical nuclear morphology, suggesting the involvement of intrinsic death pathway.

Regarding the possible involvement of 53BP2 in the cellular response to DNA damage, we have previously reported the positive correlation between the level of 53BP2 mRNA expression and the sensitivity to DNA damaging agents in various human cancer cell lines although no mutation of 53BP2 gene was detected (Mori *et al.* 2000). In addition, Ao *et al.* (2001) found that 53BP2S expression augmented the cellular apoptotic response to the DNA damage. Lopez *et al.* (2000) observed that the DNA damage induced the 53BP2 expression and protein stabilization leading to apoptosis. Bergamaschi *et al.* (2004) recently reported similar observations with ASPP2 (53BP2L). Therefore, it is likely that the activated p53 may augment the 53BP2-mediated cell death. In support of this action of p53, Marchenko *et al.* (2000) demonstrated the mitochondrial translocation of p53 upon irradiation and induction of apoptosis through the intrinsic death pathway. Mihara *et al.* (2003) further explored the mitochondrial involvement of p53 and found that p53 formed a complex with

Bcl-2 and Bcl_xL followed by permeabilization of the outer mitochondrial membrane.

Intriguingly, Iwabuchi *et al.* (1998) and Samuels-Lev *et al.* (2001) found that p53-mediated transactivation was augmented by 53BP2S and 53BP2L (ASPP2), respectively. Samuels-Lev *et al.* (2001) proposed a model that 53BP2L interacts with p53 in the nucleus and specifically enhances gene expression of p53 responsive pro-apoptotic genes such as Bax. Although the 3D structure model of p53 and 53BP2 complex (Gorina & Pavletich 1996) does not support their hypothesis because when 53BP2 binds to p53, it involves the L3 loop of p53 (required for its DNA binding) and the H1 helix (required for p53 dimerization), thus precluding the p53 binding to DNA, there may be multiple mechanisms by which 53BP2 induces apoptosis.

In addition to the possible involvement of p53 and 53BP2 in apoptosis, 53BP2 abnormality is implicated in autoimmunity such as systemic lupus erythematosus (SLE) since one of the genetic loci of the familial incidence of SLE was shown to be located to 1q42.1 (Tsao *et al.* 1997), to which *TP53BP2* is located (Yang *et al.* 1997). This is coincided with the fact that abnormalities of various apoptosis-associated factors were reported in SLE and its animal models (Fisher *et al.* 1995; Sneller *et al.* 1997; Jackson & Puck 1999). Further genetic studies are needed to find a link between 53BP2 and autoimmunity.

Our observations together with those of others suggest that 53BP2 is involved in apoptosis at multiple steps and is implicated in various pathological processes. Since 53BP2 has been shown to interact with a number of proteins responsible for the regulation of apoptosis such as p53, Bcl-2 and NF- κ B p65 subunit, selective interaction of 53BP2 with these proteins may determine the susceptibility of cells to trigger the apoptotic pathway.

Experimental procedures

Reagents and antibodies

FuGENE 6 and SuperFect transfection reagents were purchased from Roche Molecular Biochemicals (Indianapolis, IN, USA) and QIAGEN (Qiagen Inc., Valencia, CA, USA), respectively. PE-conjugated annexin V and 7-AAD (Becton Dickinson, Mountain View, CA, USA), ponasterone A (pon A) (Invitrogen, La Jolla, CA, USA) were commercially obtained. The caspase inhibitors (caspase-3 inhibitor, Z-DEVD-FMK; caspase-8 inhibitor, Z-IETD-FMK; caspase-9 inhibitor, Z-LEHD-FMK; caspase-family inhibitor, Z-VAD-FMK) were purchased from MBL. Mouse monoclonal antibodies to human

53BP2 (BD Transduction Laboratories, San Diego, CA, USA), β -tubulin (Sigma Chemical Co., St. Louis, MO, USA), human lactate dehydrogenase (LDH) (MBL, Nagoya, Japan) and human Fas (Sigma), and mouse polyclonal antibody to human mitochondrial heat shock protein 70 (Affinity Bioreagents, Golden, Colorado, USA) were purchased from individual suppliers. The rabbit polyclonal antibody to human 53BP2 was a generous gift from L. Naumovski (Stanford University, CA, USA). Mouse monoclonal antibodies to caspase-8 (cleaved form) and caspase-9 (cleaved form) and rabbit polyclonal antibody to PARP were purchased from Cell Signaling Technology (Beverly, MA, USA).

Plasmids

Construction of the 53BP2S expression plasmids, pDNA3.1-53BP2 and pEGFP-53BP2, expressing 53BP2S protein (1005 amino acids) either alone or in fusion with green fluorescence protein (GFP), was reported previously (Yang *et al.* 1999). pCEP4-ASPP2, expressing 53BP2L (1128 amino acids), was a gift from L. Naumovski. pDsRed2-Mito, expressing a fusion protein of the *Discozyma* sp. red fluorescent protein linked to the mitochondrial targeting sequence from subunit VIII of human cytochrome oxidase, was purchased from BD Bioscience Clontech (Palo Alto, CA, USA).

Cell lines and cultures

The 53BP2S inducible cell line 293/53BP2 and its control cell line 293/LZ were kindly provided by Charles D. Lopez, Stanford University, CA, USA and previously described (Lopez *et al.* 2000). These cells were grown at 37 °C in 5% CO₂ in Dulbecco's modified Eagle medium (DMEM) with 10% (v/v) heat-inactivated foetal calf serum, 290 μ g/mL of L-glutamine, 100 U/mL penicillin, 100 μ g/mL streptomycin, 600 μ g/mL G418 and 500 μ g/mL Zeocin. The parental 293 and HeLa cells were grown at 37 °C in DMEM with 10% (v/v) heat-inactivated foetal calf serum (IBL, Maebashi, Japan), 1 mM glutamate, 100 U/mL penicillin, and 100 μ g/mL streptomycin. A human pancreatic cancer cell line MIA PaCa-2 was grown in Eagle minimal essential medium supplemented with nonessential amino acids, 10% (v/v) heat-inactivated foetal calf serum, 100 U/mL penicillin, and 100 μ g/mL streptomycin.

Immunostaining

Semi-confluent MIA PaCa-2 cells on Laboratory-Tek tissue culture chamber slides were fixed with 4.5%

paraformaldehyde in PBS for 15 min at room temperature, rinsed twice with PBS, and incubated with PBS containing 0.5% Triton X-100 for 20 min at room temperature. They were subsequently incubated with the primary anti-53BP2 mouse antibody (B92320, Transduction Laboratories, Lexington, KY, USA) for 1 h at 37 °C, rinsed three times with PBS containing 0.05% Triton X-100, and incubated with the secondary antibody, rhodamine-conjugated goat anti-mouse IgG (Calbiochem-Novabiochem, La Jolla, CA, USA), for 1 h at 37 °C. The slides were rinsed with PBS for three times and mounted with buffered glycerol for fluorescent microscopic examination. Primary and secondary antibodies were diluted at 1 : 100 and 1 : 200, respectively, in PBS containing 3% bovine serum albumin.

Cell fractionation

In order to examine the cellular localization of 53BP2 in the 293/53BP2 cells, cells were pretreated with pon A (5 μ M, 48 h) and subjected to fractionation using commercial kits (Nuclear/Cytosol Fractionation Kit and Mitochondria/Cytosol Fractionation Kit, BioVision, Mountain View, CA, USA). The heavy membrane precipitate containing mitochondria was extensively washed in order to avoid the contamination of cytoplasmic proteins. The identification of 53BP2 and validation of cell fractionation were performed by Western blotting with antibodies to 53BP2, LDH (cytoplasmic marker) and mitochondrial heat shock protein 70 (mitochondria marker).

Flow cytometric analysis of apoptosis

In order to assess apoptosis, flow cytometric analysis was performed using FACScan (Becton Dickinson). MIA PaCa-2 cell were transiently transfected with pcDNA3.1-53BP2 expressing 53BP2S or pCEP4-ASPP2 expressing 53BP2L using SuperFect according to the manufacturer's recommendations. Cells at a concentration of approximately 1×10^6 cells/mL were washed twice with cold PBS and resuspended in annexin V binding buffer (10 mM HEPES-NaOH (pH 7.4), 140 mM NaCl and 2.5 mM CaCl₂). In some experiments, cells were double-stained with annexin V and 7-Amino-actinomycin D (7-AAD). 293/53BP2 cells were induced to express 53BP2 by incubation with 5 μ M pon A and apoptotic cells were similarly counted.

Microscopic examination

In order to examine the cellular localization of 53BP2S, 293 cells were cultured on 2-well Laboratory-Tek tissue

culture chamber slides and transfected with 0.4 μ g of pEGFP-53BP2 expressing 53BP2S together with 0.1 μ g of the mitochondria targeting plasmid, pDsRed2-Mito (BD Bioscience Clontech). The transfected cells were fixed with 4.0% paraformaldehyde in PBS for 15 min at room temperature, and observed under the confocal microscope (RADIANCE2000; Bio-Rad, Hercules, CA, USA). Each fluorophore was recorded separately using narrow-band filters centered at 522 nm for GFP fluorescence and 605 nm for DsRed2 fluorescence.

Evaluation of apoptosis by Western blotting

Apoptosis was also assessed by the cleavage of PARP, and caspases-8 and -9 by Western blotting using relevant antibodies described above. Briefly, whole cell extracts were lysed in 200 μ L of ice-cold lysis buffer (50 mM Tris-HCl (pH 8.0), 100 mM NaCl, 5 mM EDTA, 50 mM sodium fluoride, 2 mM dithiothreitol, 0.25% Nonidet P-40, 1 mM phenylmethyl-sulfonyl fluoride, 10 μ g/mL aprotinin, 10 μ g/mL leupeptin and 1 μ g/mL pepstatin (A). The lysate was cleared by centrifugation and the protein concentration of the whole cell extract was measured using Bio-Rad DC protein assay kit (Bio-Rad). Equal amounts of cell lysates (10 μ g protein) were resolved by 10% SDS-PAGE and transferred on nitrocellulose membrane followed by incubating with individual antibodies. The immunoreactive proteins were visualized by ECL.

Determination of mitochondrial $\Delta\Psi_m$ in cultured cells

To evaluate $\Delta\Psi_m$, cells were treated with 10 μ g/mL Rh123 for 15 min at 37 °C. After incubation, cells were washed with PBS(+) for three times, re-suspended in PBS(+), and fluorescence was scored immediately by flow cytometer. To visualize the cells with depressed $\Delta\Psi_m$, cells growing on Laboratory-Tek chambered cover glass were stained with 40 nM CMXRos in PBS(+) for 15 min, washed with PBS(+) for three times and observed under the confocal microscope (Bio-Rad MRC600UVF). The acquisitions of the mitochondrial images were provided by 585LP emission filter with same setting (Iris: 2.0, Gain: 1.4).

Acknowledgments

We thank Drs Louie Naumovski (Stanford University) for his generous gifts of 293/53BP2 cells, polyclonal antibody to 53BP2, and a plasmid expressing 53BP2L. This work was supported in part by grants-in-aid from the Ministry of Health, Labor and Welfare, the

Ministry of Education, Culture, Sports, Science and Technology of Japan and Japanese Human Sciences Foundation.

References

- Ao, Y., Rohde, L.H. & Naumovski, L. (2001) p53-interacting protein 53BP2 inhibits clonogenic survival and sensitizes cells to doxorubicin but not paclitaxel-induced apoptosis. *Oncogene* **20**, 2720–2725.
- Bergamaschi, D., Samuels, Y., Jin, B., Duraisingham, S., Crook, T. & Lu, X. (2004) ASPP1 and ASPP2: common activators of p53 family members. *Mol. Cell. Biol.* **24**, 1341–1350.
- Daniel, N.N. & Korsmeyer, S.J. (2004) Cell Death: Critical Control Points. *Cell* **116**, 205–219.
- Fisher, G.H., Rosenberg, F.J., Straus, S.E., *et al.* (1995) Dominant interfering Fas gene mutations impair apoptosis in a human autoimmune lymphoproliferative syndrome. *Cell* **81**, 935–946.
- Gorina, S. & Pavletich, N.P. (1996) Structure of the p53 tumor suppressor bound to the ankyrin and SH3 domains of 53BP2. *Science* **274**, 1001–1005.
- Green, D.R. & Reed, J.C. (1998) Mitochondria and apoptosis. *Science* **281**, 1309–1312.
- Iwabuchi, K., Bartel, P.L., Li, B., Marraccino, R. & Fields, S. (1994) Two cellular proteins that bind to wild-type but not mutant p53. *Proceedings Natl. Acad. Sci. USA* **91**, 6098–6102.
- Iwabuchi, K., Li, B., Massa, H.F., Trask, B.J., Date, T. & Fields, S. (1998) Stimulation of p53-mediated transcriptional activation by the p53-binding proteins, 53BP1 and 53BP2. *J. Biol. Chem.* **273**, 26061–26068.
- Jackson, C.E. & Puck, J.M. (1999) Autoimmune lymphoproliferative syndrome, a disorder of apoptosis. *Curr. Opin. Pediatr.* **11**, 521–527.
- Judith, H.M., Caroline, D., Jean, C.M. & James, D. (2004) Role of mitochondrial membrane permeabilization in apoptosis and cancer. *Oncogene* **23**, 2850–2860.
- Lopez, C.D., Ao, Y., Rohde, L.H., *et al.* (2000) Proapoptotic p53-interacting protein 53BP2 is induced by UV irradiation but suppressed by p53. *Mol. Cell. Biol.* **20**, 8018–8025.
- Marchenko, N.D., Zaika, A. & Moll, U.M. (2000) Death signal-induced localization of p53 protein to mitochondria. A potential role in apoptotic signaling. *J. Biol. Chem.* **275**, 16202–16212.
- Mihara, M., Erster, S., Zaika, A., *et al.* (2003) p53 has a direct apoptogenic role at the mitochondria. *Mol. Cell* **11**, 577–590.
- Mori, T., Okamoto, H., Takahashi, N., Ueda, R. & Okamoto, T. (2000) Aberrant overexpression of 53BP2 mRNA in lung cancer cell lines. *FEBS Lett.* **465**, 124–128.
- Naumovski, L. & Cleary, M.L. (1996) The p53-binding protein 53BP2 also interacts with Bcl2 and impedes cell cycle progression at G2/M. *Mol. Cell. Biol.* **16**, 3884–3892.
- Samuels-Lev, Y., O'Connor, D.J., Bergamaschi, D., *et al.* (2001) ASPP proteins specifically stimulate the apoptotic function of p53. *Mol. Cell* **8**, 781–794.
- Sneller, M.C., Wang, J., Dale, J.K., *et al.* (1997) Clinical, immunologic, and genetic features of an autoimmune lymphoproliferative syndrome associated with abnormal lymphocyte apoptosis. *Blood* **89**, 1341–1348.
- Takahashi, N., Kobayashi, S., Jiang, X., *et al.* (2004) Expression of 53BP2 and ASPP2 proteins from TP53BP2 gene by alternative splicing. *Biochem. Biophys. Res. Commun.* **315**, 434–438.
- Tsao, B.P., Canto, R.M., Kalunian, K.C., *et al.* (1997) Evidence for Linkage of a Candidate Chromosome 1 Region to Human Systemic Lupus Erythematosus. *J. Clin. Invest.* **99**, 725–731.
- Yang, J.P., Hori, M., Takahashi, N., Kawabe, T., Kato, H. & Okamoto, T. (1999) NF- κ B subunit p65 binds to 53BP2 and inhibits cell death induced by 53BP2. *Oncogene* **18**, 5177–5186.
- Yang, J.P., Ono, T., Sonta, S., Kawabe, T. & Okamoto, T. (1997) Assignment of p53 binding protein (TP53BP2) to human chromosome band 1q42.1 by in situ hybridization. *Cytogenet. Cell Genet.* **78**, 61–62.

Received: 8 October 2004

Accepted: 12 December 2004

Growth Inhibition of Multiple Myeloma Cells by a Novel I κ B Kinase Inhibitor

Takaomi Sanda,^{1,2} Shinsuke Iida,²
Hiroka Ogura,¹ Kaori Asamitsu,¹ Toshiki Murata,³
Kevin B. Bacon,⁴ Ryuzo Ueda,²
and Takashi Okamoto¹

Departments of ¹Molecular and Cellular Biology, and ²Internal Medicine and Molecular Science, Nagoya City University Graduate School of Medical Sciences, Nagoya, Japan and Departments of ³Chemistry and ⁴Biology, Research Center Kyoto, Bayer Yakuhin, Ltd., Kyoto, Japan

ABSTRACT

Involvement of nuclear factor- κ B (NF- κ B) in cell survival and proliferation of multiple myeloma has been well established. In this study we observed that NF- κ B is constitutively activated in all human myeloma cell lines, thus confirming the previous studies. In addition, we found the phosphorylation of p65 subunit of NF- κ B in addition to the phosphorylation of I κ B α and the activation of NF- κ B DNA binding and that various target genes of NF- κ B including *bcl-xL*, *XIAP*, *c-IAP1*, *cyclin D1*, and *IL-6* are up-regulated. We then examined the effect of a novel I κ B kinase inhibitor, 2-amino-6-[2-(cyclopropylmethoxy)-6-hydroxyphenyl]-4-piperidin-4-yl nicotinonitrile (ACHP). When myeloma cells were treated with ACHP, the cell growth was efficiently inhibited with IC₅₀ values ranging from 18 to 35 μ mol/L concomitantly with inhibition of the phosphorylation of I κ B α /p65 and NF- κ B DNA-binding, down-regulation of the NF- κ B target genes, and induction of apoptosis. In addition, we observed the treatment of ACHP augmented the cytotoxic effects of vincristine and melphalan (L-phenylalanine mustard), conventional antimyeloma drugs. These findings indicate that I κ B kinase inhibitors such as ACHP can sensitize myeloma cells to the cytotoxic effects of chemotherapeutic agents by blocking the antiapoptotic nature of myeloma cells endowed by the constitutive activation of NF- κ B.

INTRODUCTION

Multiple myeloma is an intractable B-cell malignancy characterized by clonal proliferation of a terminally differentiated plasma cell in bone marrow associated with monoclonal hyper-

gammaglobulinemia and multiple osteolytic bone lesions (1, 2). Although recent combination chemotherapy, using melphalan [L-phenylalanine mustard (PAM)], vincristine, and corticosteroids, can induce complete remission in multiple myeloma patients, the long-term remission is hardly attainable mostly due to the frequent acquisition of drug resistance and low adherence (1). Therefore, novel treatment modality has been intensively investigated.

It is noted that the interaction between myeloma cells and bone marrow stromal cells plays a crucial role through the production of cytokines or growth factors and the cognate binding of adhesion molecules (1). Among various cytokines and growth factors, interleukin-6 (IL-6) and vascular endothelial growth factor were reported to stimulate myeloma cell proliferation and its migration (3). The establishment of such bone marrow microenvironment conceivably accelerates cell proliferation. In other words, a limited number of genes including IL-6, vascular endothelial growth factor, and adhesion molecules are the principal pathophysiologic determinants of multiple myeloma. Interestingly, gene expression of these genes is under the control of a common transcription factor, nuclear factor- κ B (NF- κ B; refs. 1, 4). Moreover, extracellular stimuli for the growth of myeloma cells, such as CD40 ligand (CD40L) expressed on activated T cells, insulin-like growth factor I, and tumor necrosis factor α (TNF α), are known to promote the NF- κ B activation pathway at various steps (5-7). A similar effect of NF- κ B is also noted in other malignancies including adult T-cell leukemia (8), chronic lymphocytic leukemia (9), activated B-cell diffuse large B-cell lymphoma (9), Hodgkin's disease (9), hepatocellular carcinoma (10), and colorectal cancer (11). In fact, NF- κ B inhibitors were found effective in the treatment of some cancers (12). Thus, NF- κ B and its signal transduction pathway are considered as the feasible molecular target for novel cancer therapy.

NF- κ B is a hetero- or homodimer consisting of Rel family proteins, p65 (RelA), RelB, c-Rel, p50/p105, and p52/p100, and normally present in the cytoplasm in association with its inhibitor, I κ B (13). Stimulation by the inflammatory cytokines such as TNF α and IL-1 β results in the activation of I κ B kinase (IKK) complex through mitogen-activated protein kinase/extracellular signal-regulated kinase kinase 1,3 or NF- κ B-inducing kinase (14, 15). IKK is a large molecular weight complex consisting of three subunits, IKK α , IKK β , and IKK γ /NEMO, in which IKK α and IKK β serve as catalytic subunits that phosphorylate I κ B α on two serine residues (Ser32/Ser36; refs. 16-18). Recent reports by us and others have shown that IKK α also phosphorylates p65 at Ser536, which is crucial for the transcriptional competence of NF- κ B when bound to the promoter sequence of target genes in the nucleus (19, 20).

In this study, we examined the effect of a novel IKK inhibitor, 2-amino-6-[2-(cyclopropylmethoxy)-6-hydroxyphenyl]-4-piperidin-4-yl nicotinonitrile (ACHP), on the growth and survival of myeloma cell lines. This compound was initially synthesized by Murata et al. (21) based on the massive

Received 9/22/04; revised 11/19/04; accepted 12/6/04.

Grant support: Ministry of Education, Culture, Sports, Science, and Technology, and the Ministry of Health, Labor, and Welfare of Japan. The costs of publication of this article were defrayed in part by the payment of page charges. This article must therefore be hereby marked advertisement in accordance with 18 U.S.C. Section 1734 solely to indicate this fact.

Requests for reprints: Takashi Okamoto, Department of Molecular and Cellular Biology, Nagoya City University Graduate School of Medical Sciences, 1 Kawasumi, Mizuho-cho, Mizuho-ku, Nagoya, Aichi 467-08601, Japan. Phone: 81-52-853-8205; Fax: 81-52-859-1235; E-mail: tokamoto@med.nagoya-cu.ac.jp.

©2005 American Association for Cancer Research.

screening. Among these compounds, ACHP exhibited the highest selectivity for IKK β and IKK α (IC₅₀ values for IKK β and IKK α are 8.5 and 250 nmol/L, respectively, measured by *in vitro* kinase assays) over other kinases such as IKK3, Syk, and mitogen-activated protein kinase kinase 4 (IC₅₀ > 20 μ mol/L for these kinases; ref. 22). In addition, ACHP showed good aqueous solubility and cell-permeability, thus demonstrating a very high oral bioavailability in mice and rats.

Here we show that I κ B α and p65 are constitutively phosphorylated in myeloma cells, indicating the persistent activation of NF- κ B, and ACHP could efficiently block NF- κ B pathway in myeloma cells, thus arresting cell growth and inducing apoptotic cell death. An apparent synergism was also detected between ACHP and other conventional anticancer drugs used in the treatment of myeloma.

MATERIALS AND METHODS

Cell Lines

Human myeloma cell lines, ILKM-2, ILKM-3, KM5, U266, NCUMM-2, AMO1, and NOP1, and a B-cell lymphoma cell line, BJAB, were used in this study as described previously (23). These cell lines were cultured in RPMI 1640 supplemented with 10% fetal bovine serum, streptomycin, and penicillin at 37°C in 5% CO₂ incubator. Exogenous IL-6 is required for the growth of ILKM-2 and ILKM-3, whereas other cell lines can grow without exogenous IL-6. U266 cells produce IL-6 in an autocrine fashion. Although U266 and BJAB cells are known to have constitutively activated NF- κ B (24, 25), constitutive activation of NF- κ B has not been definitively reported in other cell lines.

Reagents

The novel IKK inhibitor, ACHP, was a kind gift from Bayer Yakuhin (Kyoto, Japan). Melphalan (PAM), vincristine, and dexamethasone were obtained from Sigma (St. Louis, MO). PAM was dissolved in dimethyl sulfoxide whereas vincristine and dexamethasone were resolved in PBS. In each experiment, equal amounts of dimethyl sulfoxide or PBS were added to control cells. We confirmed that dimethyl sulfoxide concentrations used in this study did not affect cell viability (data not shown). Human recombinant TNF α was purchased from Roche (Mannheim, Germany) and used at 5 ng/mL for NF- κ B stimulation. Recombinant human IL-6 (Diaclone Research, Besancon, France) was added at a final concentration of 10 ng/mL.

Immunoblot Analysis

For analysis of various proteins, $\sim 1.0 \times 10^6$ cells were maintained with or without ACHP at 37°C. These cells were washed once with cold PBS and resuspended in 50 μ L of hypotonic lysis buffer [20 mmol/L HEPES-KOH (pH 7.9), 10 mmol/L KCl, 1 mmol/L EDTA, 1 mmol/L Na₃VO₄, 5 mmol/L NaF, 1 mmol/L phenylmethylsulfonyl fluoride, 0.2% Triton X-100, protease inhibitor]. After 20 minutes of incubation on ice, the samples were centrifuged and the supernatant was collected as cytoplasmic extract. Protein concentration was measured using detergent-compatible protein assay (Bio-Rad, Hercules, CA) and equal amounts of the proteins were electrophoresed on 10% SDS-PAGE and transferred onto the nitrocellulose membrane. The membranes were blocked with TBS-T [10 mmol/L Tris-HCl (pH 8.0), 15 mmol/L NaCl, 0.1%

Tween 20] containing 5% nonfat milk for 2 hours at room temperature, and incubated with TBS-T containing 5% nonfat milk and 1:1,000 diluted antibodies against either phospho-I κ B- α (Ser32) or phospho-p65 (Ser536; Cell Signaling Technology, Beverly, MA) overnight at 4°C. For antibodies against p65, p52/p100, I κ B- α , and α -tubulin (Santa Cruz, Santa Cruz, CA), incubation was done at room temperature for 2 hours. After incubation, the membranes were rinsed with TBS-T and further incubated with horseradish peroxidase-conjugated secondary antibodies (Amersham Biosciences, Buckinghamshire, United Kingdom) in TBS-T with 5% nonfat milk at room temperature for 1 hour. Each protein was detected by chemiluminescence using SuperSignal (Pierce, Rockford, IL).

Electrophoretic Mobility Shift Assay

Electrophoretic mobility shift assay was done as described previously (26). Briefly, 1.0×10^6 cells were cultured with or without ACHP at 37°C, washed with PBS, and treated with hypotonic lysis buffer. After 20 minutes of incubation on ice, the cells were centrifuged to remove supernatant and resuspended in 50 μ L of hypertonic lysis buffer [50 mmol/L HEPES-KOH (pH 7.9), 400 mmol/L NaCl, 1 mmol/L EDTA, 1 mmol/L Na₃VO₄, 5 mmol/L NaF, 1 mmol/L phenylmethylsulfonyl fluoride, 0.2% Triton X-100, protease inhibitor]. Thirty minutes after incubation at 4°C, the supernatant was collected as nuclear extract. Electrophoretic mobility shift assay was done using double stranded oligonucleotides containing the κ B sequence taken from HIV long terminal repeat (5'-TGT CGA ATG CAA ATC ACT AGA A-3'). The probe DNA was 5' end-labeled using T4 polynucleotide kinase and [γ -³²P]-ATP (Amersham Biosciences). DNA binding reactions were done at 30°C for 15 minutes with labeled DNA and 25 μ g nuclear extract in 20 μ L binding buffer [22 mmol/L HEPES-KOH (pH 7.9), 80 mmol/L KCl, 5% glycerol, 0.1% NP40, 1 mmol/L DTT, 2 μ g poly dI-dC, 2 μ g tRNA, and protease inhibitor]. The samples were loaded on 5% nondenaturing polyacrylamide gel with 0.5 \times Tris-Borate-EDTA buffer at 4°C, followed by autoradiography.

Transient Luciferase Assay

Approximately 2.0×10^6 /well U266 cells were transfected in 12-well plates in triplicates using DEMRIE-C reagent (Invitrogen, Carlsbad, CA) according to the recommendation of the manufacturer. For each transfection, 2.5 μ g of reporter plasmid, 4 κ Bwt-Luc, or 4 κ Bmut-Luc, and 1.5 μ g of the internal control plasmid, pRL-TK, expressing Renilla luciferase, were used. The construction of these plasmids was described previously (26). Twenty-four hours after transfection, the cells were treated with ACHP. After 4 hours of incubation, the cells were harvested and the luciferase activity was measured by luminometer as described (27). The cells were treated with TNF α and harvested after 30 minutes of treatment. The luciferase activity was normalized with Renilla luciferase activity used as an internal control. The efficiency of transfection was about 0.9% as estimated from the experiment with a plasmid expressing green fluorescent protein (data not shown).

Reverse Transcription-PCR

To detect mRNA expression of various genes, 1.0×10^6 cells in 1 mL were maintained at 37°C in CO₂ incubator, washed once

with PBS, homogenized with QIAshredder (Qiagen, Alameda, CA), and total RNA was purified using RNeasy (Qiagen) according to the protocol of the manufacturer. After incubation with DNase I (Invitrogen), 1 μ g of total RNA was reverse transcribed using SuperScript First-Strand synthesis System (Invitrogen). One-seventh of each sample was subjected to PCR amplification for 33 cycles, and the products were analyzed by agarose gel electrophoresis. The oligonucleotide primers were as follows: *bcl-2*, sense 5'-TCG CTA CCG TCG TGA CTT C-3' and antisense, 5'-AAA CAG AGG TEG CAT GCT.G-3'; *bcl-xL*, sense 5'-GTT GTA CCT GCT TGC TGT CGC CGG-3' and antisense 5'-AGC TTG TAG GAG AGA AAG TCG ACC-3'; *cyclin D1*, sense 5'-CCC TCG GTG TCC TAC TTC AAA-3' and antisense 5'-CAC CTC CTC CTC CTC TTC-3'; *XIAP*, sense 5'-CTT GCATAC TGT CTT TCT GAG C-3' and antisense, 5'-ACA CCATAT ACC CGA GGA AC-3'; *c-IAP1*, sense 5'-CCT GTG GTT AAA TCT GCC TTG-3' and antisense 5'-CAA TTC GGC ACC ATA ACT CTG-3'; *β -actin*, sense CCA GGC ACC AGG GCG TGA TG-3' and antisense 5'-CGG CCA GCC AGG TCC AGA CG-3'.

Interleukin-6 Production Assay

To measure IL-6 production, 2.0×10^5 of U266 cells in 500 μ L medium were cultured at 37°C for 48 hours, centrifuged to collect supernatant, and the IL-6 concentrations were determined using ELISA kit according to the instruction of the manufacturer (Amersham Biosciences).

Growth Inhibition Assay

Growth inhibitory effects of compounds were analyzed using 3-(4,5-dimethylthiazol-2-yl)-2,5-diphenyltetrazolium bromide assay (27). Approximately 1.0×10^4 to 1.5×10^4 cells (in 100 μ L/well) were cultured in 96-well plates in triplicates in the presence or absence of each reagent or in combination at 37°C. After incubation, 10 μ L (5 mg/mL) of 3-(4,5-dimethylthiazol-2-yl)-2,5-diphenyltetrazolium bromide solution (Sigma) were added to each well, the cells were incubated for 4 hours at 37°C, and 100 μ L of lysis buffer (0.04 mol/L HCl, isopropanol) were added. Absorbances at 570 and 630 nm were measured with the aid of multiplate reader using plain medium as blank. Cell viability (%) was calculated as follows: $(A_{630} - A_{570} \text{ of the samples} / A_{630} - A_{570} \text{ of the control}) \times 100$ (%).

Cell Cycle Analysis

Cytofluorometric analysis was done with $\sim 1.0 \times 10^6$ cells as previously described (28). After incubation with or without ACHP, the cells were washed with cold PBS and fixed with 70% ethanol at -30°C overnight. The cell pellets were resuspended in 500 μ L PBS containing 2 mg/mL RNase A (Roche) and kept at 37°C for 30 minutes. Then, the cell pellets were resuspended in 500 μ L PBS containing 20 mg/mL propidium iodide (PI) followed by incubation at room temperature for 30 minutes. The DNA content of each cell preparation was analyzed by flow cytometry (FACScan, BD Bioscience, San Jose, CA) using CellQuest analysis program.

Apoptosis Assay

Briefly, cells undergoing apoptosis were detected as previously reported (29). After treating the cells (2.0×10^5 cells)

at 37°C with or without ACHP for 8 hours, the cells were washed with cold PBS and resuspended in staining buffer containing PI and FITC-conjugated Annexin V (MEBCYTO apoptosis kit, MBL, Nagoya, Japan). After 20 minutes of incubation in the dark at room temperature, the cells were analyzed by flow cytometry.

RESULTS

Constitutive Phosphorylation of I κ B α and p65 in Myeloma Cell Lines

In order to see the status of NF- κ B signaling in myeloma cells, we examined the phosphorylation of I κ B α and p65 subunit in a number of myeloma cell lines and BJAB B-cell line. As shown in Fig. 1, the phosphorylation of I κ B α at Ser32 was detected in most of the cell lines examined, especially in U266, ILKM-2, NCUMM-2, and BJAB. The upper bands, corresponding to heavily phosphorylated I κ B α , were detected in ILKM-2 and NCUMM-2. In addition, p65 is phosphorylated at Ser536 in all the cell lines examined. This constitutive phosphorylation of I κ B α was observed even when cells were cultured in serum-free medium (data not shown). These findings suggest that NF- κ B is constitutively activated in myeloma cells.

Constitutive Activation of Nuclear Factor- κ B DNA Binding and Inhibition by 2-Amino-6-[2-(Cyclopropylmethoxy)-6-Hydroxyphenyl]-4-Piperidin-4-yl Nicotinonitrile

We then examined if NF- κ B DNA-binding is constitutively activated in these myeloma cells by electrophoretic mobility shift assay. Representative results are shown in Fig. 2 with U266 and NCUMM-2 cells, in which the NF- κ B DNA-binding is constitutively activated. We also examined the effect of ACHP on the NF- κ B DNA binding in these cells and found that ACHP, specific inhibitor of IKK α and IKK β , could inhibit the DNA binding activity of NF- κ B (Fig. 2B). The inhibitory effect was

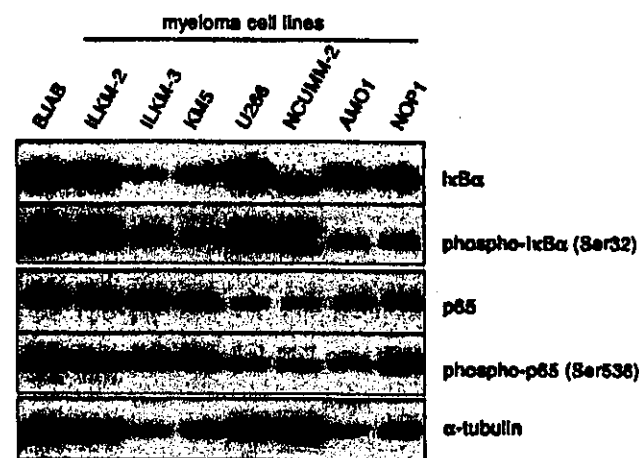


Fig. 1 Constitutive phosphorylation of I κ B α and p65 in myeloma cell lines. The cytoplasmic extracts obtained from seven myeloma cell lines (U266, ILKM-2, NCUMM-2, ILKM-3, KM5, AMO1, and NOP1) and a B-cell line (BJAB), maintained in culture without any stimulation, were examined by Western blotting analyses with specific antibodies against I κ B α , phospho-I κ B α (at Ser32), p65, and phospho-p65 (at Ser536). Anti- α -tubulin antibody was used as an internal control. The mobility shift of the phosphorylated I κ B α is noted in ILKM-2 and NCUMM-2 cells, suggesting phosphorylation at multiple sites.

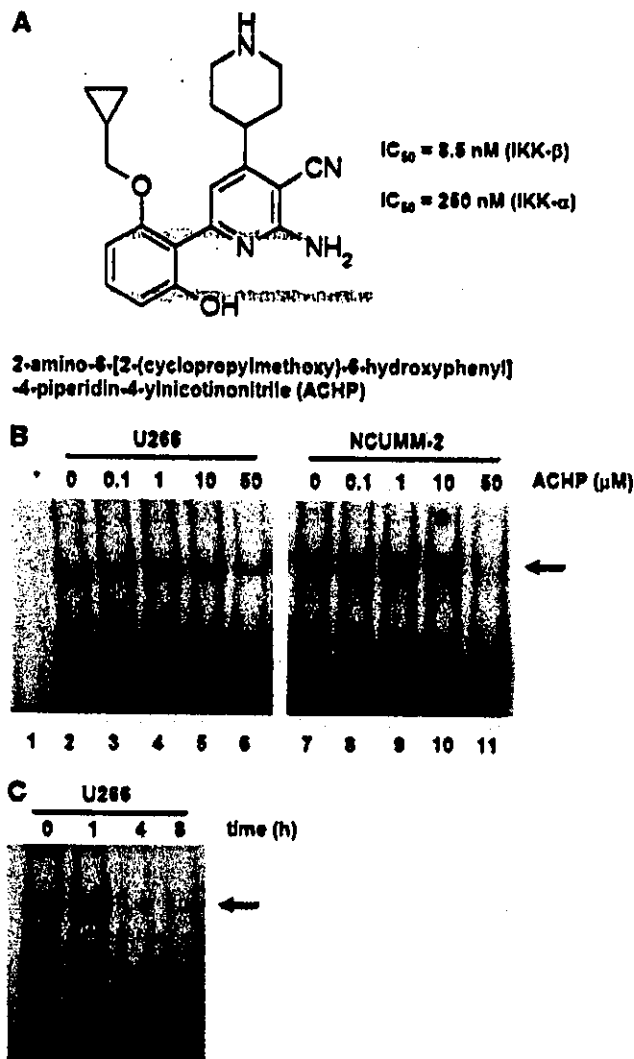


Fig. 2 Constitutive activation of NF- κ B DNA binding in myeloma cells and inhibitory effect of ACHP. **A**, structure of ACHP. **B**, dose-dependent inhibition of NF- κ B DNA binding by ACHP. The myeloma cell lines, U266 and NCUMM-2, were cultured in the absence of any stimulation and treated with ACHP (0-50 $\mu\text{mol/L}$) for 4 hours. Nuclear extracts were prepared and subjected to electrophoretic mobility shift assay. Arrow, location of the DNA-NF- κ B complex, which was confirmed by the competition assay using unlabelled κ B DNA probe and the supershift assay using antibodies for NF- κ B subunits (data not shown). Lane 1, probe DNA only; lanes 2-6 and 7-11, fixed amounts (~25 μg) of nuclear extracts from U266 and NCUMM-2 cells, respectively, were incubated with the DNA probe. The indicated concentrations of ACHP were added in cell cultures for 4 hours before preparation of the nuclear extract. **C**, time-dependent inhibition of NF- κ B DNA binding by ACHP. U266 cells were treated with ACHP (50 $\mu\text{mol/L}$) for 0 to 8 hours before preparation of the nuclear extract.

observed at ACHP concentrations greater than 10 $\mu\text{mol/L}$, and was evident after only 4 hours of treatment with ACHP (Fig. 2C).

Inhibition of IκBα and p65 Phosphorylation by 2-Amino-6-[2-(Cyclopropylmethoxy)-6-Hydroxyphenyl]-4-Piperidin-4-yl Nicotinonitrile

We then examined the effect of ACHP on the phosphorylation of IκBα and p65. As shown in Fig. 3A, ACHP efficiently

inhibited the phosphorylation of IκBα and p65 at 1 $\mu\text{mol/L}$, and phosphorylated forms of these proteins disappeared at higher concentrations. This inhibitory action was observed as early as 20 minutes after treatment (Fig. 3B). No effect of ACHP on the processing of p100/p52, another subunit of NF- κ B, was observed. Similar effects of ACHP were observed with other myeloma cell lines (data not shown).

Effect of 2-Amino-6-[2-(Cyclopropylmethoxy)-6-Hydroxyphenyl]-4-Piperidin-4-yl Nicotinonitrile on the Tumor Necrosis Factor α -mediated Nuclear Factor- κ B Transactivation

We then examined the inhibitory effect of ACHP on NF- κ B transactivation activity. By transfection of NF- κ B-dependent luciferase reporter plasmid to U266 cells, ~4-fold increase in the extent of gene expression was observed (Fig. 4A). When cells were pretreated with ACHP 4 hours before the stimulation with TNF α , a dose-dependent inhibition of gene expression was observed. The inhibitory action was evident at 0.1 $\mu\text{mol/L}$

F4

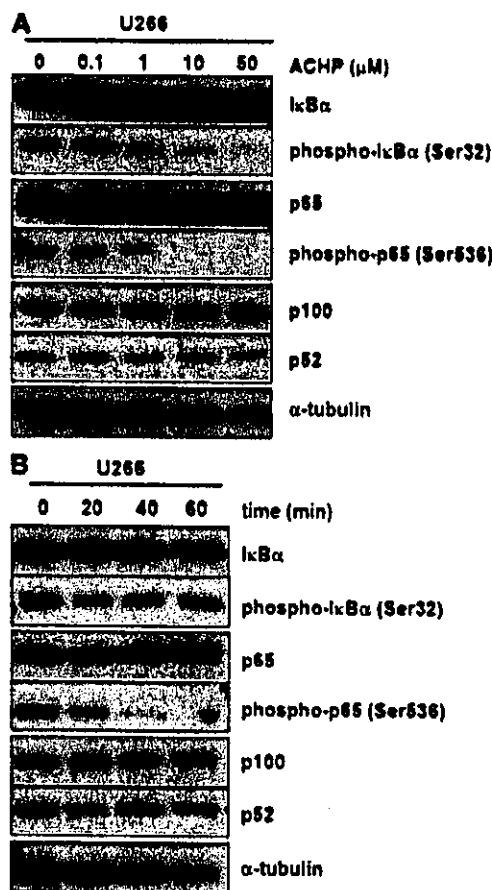


Fig. 3 Inhibition of IκBα and p65 phosphorylation by ACHP. **A**, dose-dependent inhibition by ACHP. U266 cells were treated with ACHP (0-50 $\mu\text{mol/L}$) for 20 minutes. Cytoplasmic extracts were prepared and subjected to immunoblots with the indicated antibodies. The IC_{50} values for phospho-IκBα and phospho-p65 were 1.0 and 7.6 $\mu\text{mol/L}$, respectively. **B**, time-dependent inhibition of IκBα and p65 phosphorylation by ACHP. U266 cells were treated with ACHP (10 $\mu\text{mol/L}$) for 0 to 60 minutes and the nuclear extract was obtained for the immunoblot analyses.

F3

ACHP. No such effect of ACHP was observed in control transcription using a reporter plasmid devoid of NF- κ B binding sites.

Inhibition of Gene Expressions of *cyclin D1*, *bcl-x_L*, *XIAP*, and *c-IAP1* by 2-Amino-6-[2-(Cyclopropylmethoxy)-6-Hydroxyphenyl]-4-Piperidin-4-yl Nicotinonitrile

In myeloma cells, constitutive NF- κ B activation and transcriptional induction of target antiapoptotic genes such as *bcl-x_L*, *XIAP*, and *c-IAPs* are ascribable to the resistance to apoptotic stimuli by anticancer agents (30, 31). In addition, NF- κ B also contributes to cell proliferation of myeloma cells by up-regulating growth-promoting genes such as *cyclin D1* (30). We thus examined the effect of ACHP on gene expression of these genes. As shown in Fig. 4B, whereas gene expression levels of β -actin (control) were not changed by the treatment of U266 with ACHP, inhibition of gene expressions of *bcl-x_L*, *XIAP*, *c-IAP1*, and *cyclin D1* was observed. The expression of *bcl-2* was not remarkably affected by ACHP. The inhibitory action of ACHP was observed after 4 hours (Fig. 4C). Similar results were observed with NCUMM-2 and ILKM-2 cells (data not shown). Moreover, the effect of ACHP on the production of a growth promoting cytokine, IL-6, was examined with IL-6-secreting myeloma cell line, U266. As shown in Fig. 4D, a significant reduction of IL-6 was evident at concentrations of ACHP greater than 0.1 μ mol/L. Increasing concentration of ACHP resulted in further reduction of IL-6 production associated with repression of cell growth.

Suppression of Cell Cycle Progression and Induction of Apoptosis by 2-Amino-6-[2-(Cyclopropylmethoxy)-6-Hydroxyphenyl]-4-Piperidin-4-yl Nicotinonitrile

When U266 and NCUMM-2 cells were treated with 10 μ mol/L ACHP for 24 hours, cell cycle progression was affected. As shown in Fig. 5A, whereas 24% of U266 cells were at S phase, only 17.0% of U266 cells were at S phase after treatment with ACHP. Similar results were obtained with NCUMM-2 cells. ACHP also induced apoptosis in myeloma cell lines. In Fig. 5B, the number of cells undergoing apoptosis (Annexin V (+) and PI (-)) was measured. Although the sensitivity of apoptosis to ACHP varied among different cell lines, ACHP could efficiently induce cell death. For example, in U266 cells, which were relatively resistant to the ACHP-induced apoptosis, 50 μ mol/L ACHP treatment increased the fraction of apoptotic cells from 4.2% (no treatment) to 16.0%. In NCUMM-2 cells, even a lower concentration of ACHP (10 μ mol/L) could efficiently induce apoptosis (15.8%) and a higher concentration of ACHP (50 μ mol/L) induced apoptosis in 43.7% of the cells. These findings illustrate the effect of ACHP in down-regulating antiapoptotic genes (Fig. 4).

Growth Inhibitory Effects of 2-Amino-6-[2-(Cyclopropylmethoxy)-6-Hydroxyphenyl]-4-Piperidin-4-yl Nicotinonitrile

We then assessed the net effects of ACHP on the growth of myeloma cell lines (U266, NCUMM-2, and ILKM-2) and B-cell line (BJAB). As shown in Fig. 6A, ACHP inhibited cell growth in a dose-dependent manner with mean IC₅₀ of 26.8 μ mol/L in three myeloma cell lines. There was a sharp decline in cell growth

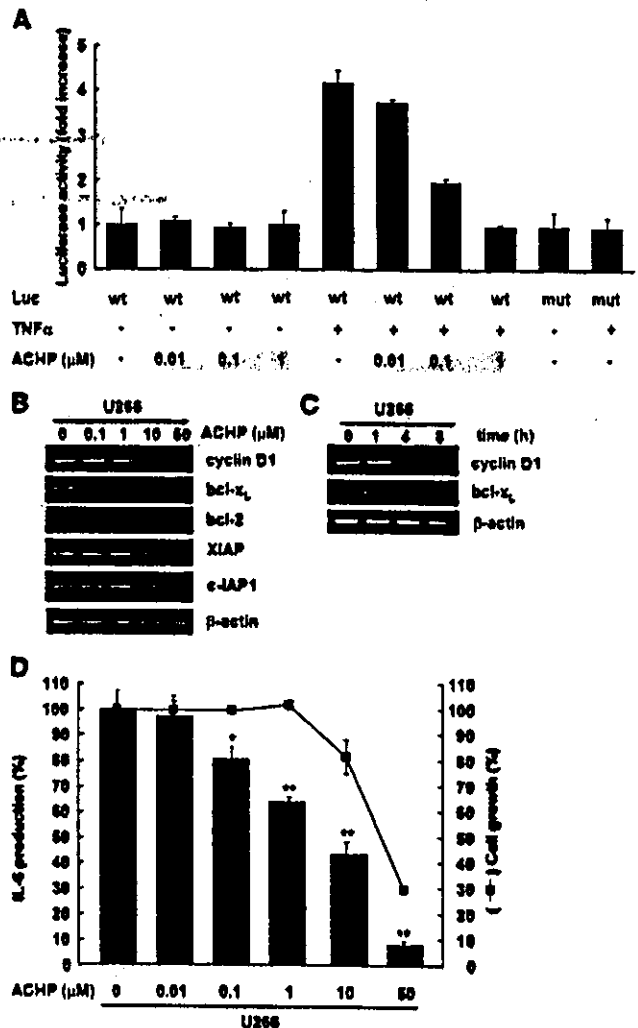


Fig. 4 Inhibition of the NF- κ B dependent transactivation and gene expression by ACHP. Luciferase reporter plasmid containing wild-type NF- κ B binding sequence (wt) or its mutant (mut) was transfected into U266 cells together with an internal control plasmid (pRL-TK). Forty hours after transfection, the cells were treated with ACHP (0-1 μ mol/L) for 4 hours, stimulated by TNF α (5 μ g/mL) for 30 minutes, and harvested for luciferase assay. The luciferase activity is indicated as fold increase compared with the untreated control (=1.0). Transfection efficiency was ~0.9% as evaluated by green fluorescent protein assay (data not shown). Experiments were done in triplicates; columns, mean; bars, SD. **B**, dose-dependent inhibition by ACHP. After U266 cells were treated with ACHP (0-50 μ mol/L) for 4 hours, total RNA samples were prepared for reverse transcription-PCR, and the mRNA levels of *cyclin D1*, *bcl-x_L*, *bcl-2*, *XIAP*, *c-IAP1*, and β -actin were examined with specific primers. **C**, time-dependent inhibition by ACHP. U266 cells were treated with ACHP (50 μ mol/L) for 0 to 8 hours, total RNA samples were prepared, and the mRNA level of each gene was assessed by reverse transcription-PCR. **D**, down-regulation of IL-6 production by ACHP. U266 cells were incubated in the presence of ACHP (0-50 μ mol/L) for 48 hours and the IL-6 levels in the supernatant were measured by ELISA method (solid bar). The effect of ACHP on the net cell growth was examined by 3-(4,5-dimethylthiazol-2-yl)-2,5-diphenyltetrazolium bromide assay (square). The results are expressed as percentage compared with the untreated control. Experiments were done in triplicates; columns, mean; bars, SD. *, $P = 0.05$; **, $P < 0.01$.

F5

F6

property between 10 and 50 μmol/L of ACHP in most of the cells, which corresponded with the effective ACHP concentration that inhibited expression of antiapoptotic genes (Fig. 4). Figure 6B shows the time course of cell growth property of U266 cells with various concentrations of ACHP. Higher concentrations of ACHP were necessary to inhibit cell growth. Lower ACHP concentrations (10 μmol/L and below) eventually allowed myeloma cells to grow for a longer time. Similar observations were obtained with other myeloma cells examined (data not shown).

Effects of 2-Amino-6-[2-(Cyclopropylmethoxy)-6-Hydroxyphenyl]-4-Piperidin-4-yl Nicotinonitrile with Other Antimyeloma Agents

Finally, we examined the feasibility of ACHP as an adjuvant chemotherapeutic agent in myeloma treatment. In the experiments described in Fig. 6C, U266 cells were cultured in the presence of PAM, vincristine, and dexamethasone together

with ACHP and the effects on cell growth were assessed. Although 10 μmol/L of ACHP alone did not efficiently inhibit U266 cell growth (Fig. 6A), combination with either PAM, vincristine, or dexamethasone showed more than additive effects in blocking cell growth in a dose-dependent manner (Fig. 6C). When cell cultures were maintained for up to 5 days, a greater effect was observed with vincristine and ACHP (Fig. 6D). Although similar effects were observed with PAM and ACHP for the first 3 days, the synergistic effect was diminished after 5 days, presumably due to the short half-life of PAM.

DISCUSSION

In spite of a significant advancement in conventional chemotherapy and wider applicability of high-dose treatment with transplantation of hematopoietic stem cells, multiple myeloma still remains incurable (3). Thus, the pursuit for novel

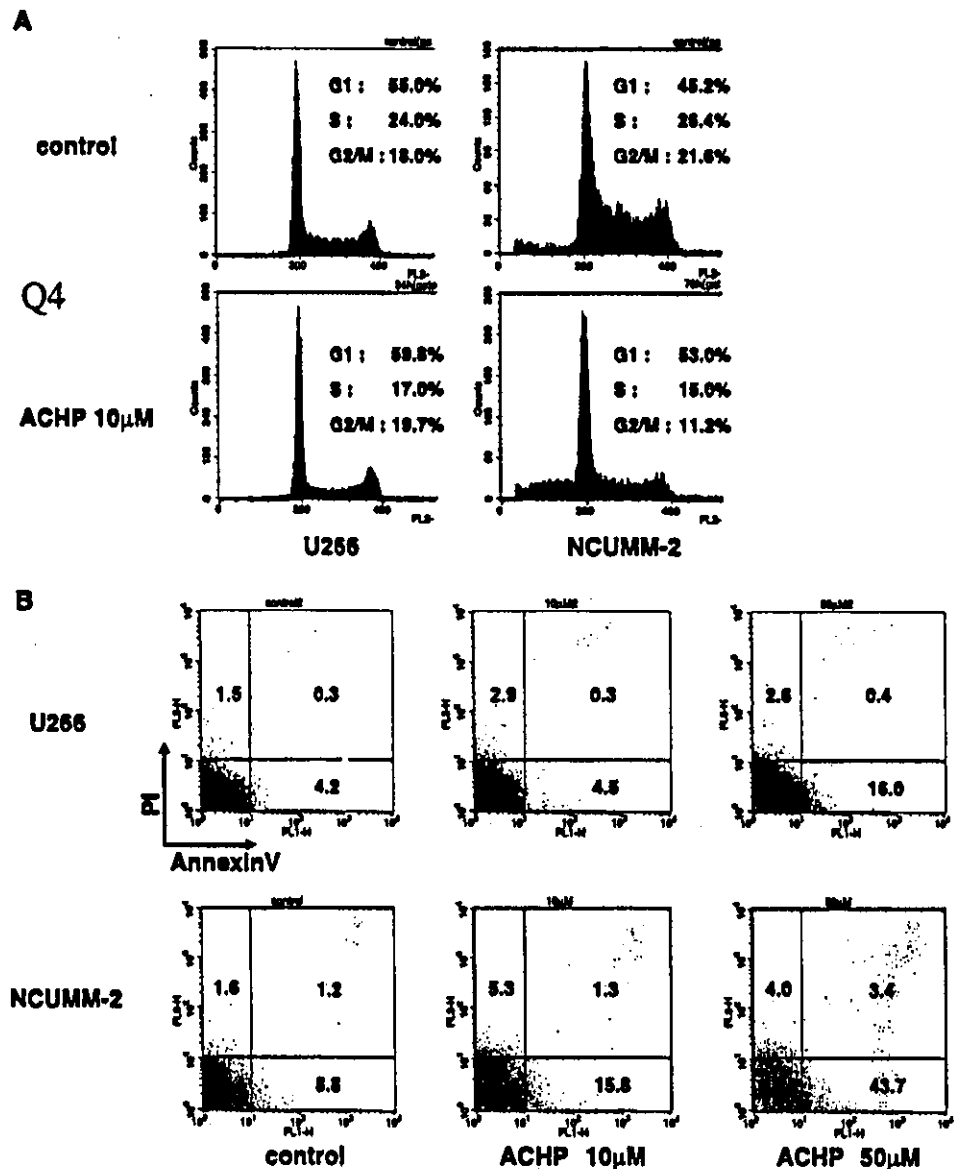
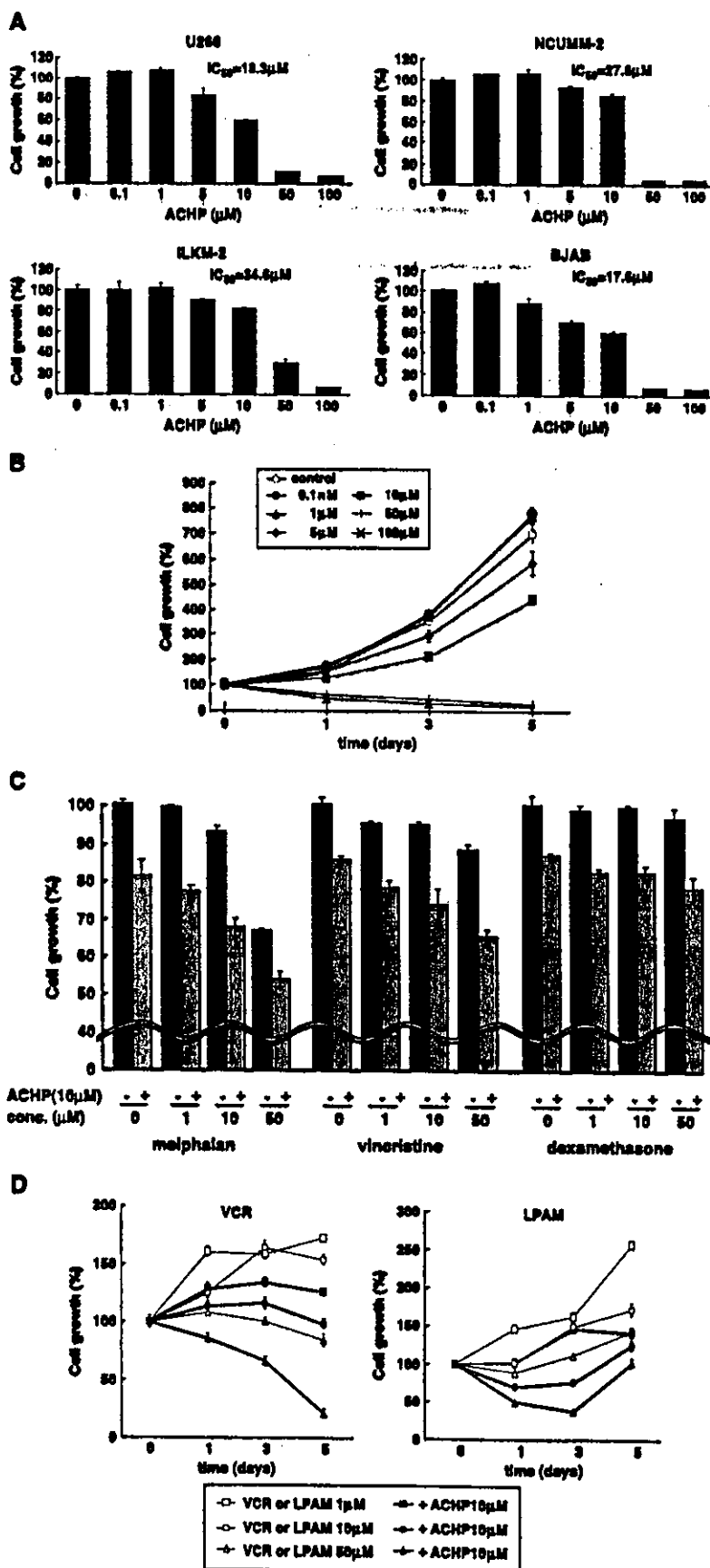


Fig. 5 Effects of ACHP on cell cycle and induction of apoptosis. **A**, inhibition of cell cycle progression by ACHP. U266 and NCUMM-2 cells were treated with ACHP (10 μmol/L) for 24 hours. Cells were stained with PI and subjected to flow cytometric analysis. The fractions of each cell cycle phase (%) are shown as percentage using the CellQuest analysis program. **B**, induction of apoptotic cells by ACHP. U266 and NCUMM-2 cells were treated with ACHP (0, 10, and 50 μmol/L) for 8 hours, stained with FITC-conjugated Annexin V and PI, and analyzed by flow cytometry. Normal cells do not stain with Annexin V or PI, whereas apoptotic cells stain with Annexin V but not PI. The percentage of each fraction is indicated.

Fig. 6 Growth inhibitory effects of ACHP. Cell growth was monitored by 3-(4,5-dimethylthiazol-2-yl)-2,5-diphenyltetrazolium bromide assay. The results are indicated as percentage compared with the untreated control or day 0. Experiments were done in triplicates; columns, mean; bars, SD. **A**, cell growth analysis of myeloma cell lines and the inhibitory effects of ACHP. Each myeloma cell and BJAB was treated with the indicated concentrations of ACHP for 3 days. **B**, effects of ACHP on the temporal profiles of U266 cell growth. U266 cells were treated with indicated concentrations of ACHP (0-100 $\mu\text{mol/L}$) up to 5 days. **C**, synergistic effects of ACHP with other antimyeloma agents. The U266 myeloma cells were cultured with indicated concentrations of antimyeloma agents in the absence or presence (10 $\mu\text{mol/L}$) of ACHP for 1 day. **D**, the temporal profile of U266 cells. The combined effects of ACHP and vincristine or PAM. U266 cells were cultured with vincristine or PAM (1-50 $\mu\text{mol/L}$) and combined with ACHP (10 $\mu\text{mol/L}$) for up to 5 days. Cell growth was assessed at day 1, day 3, and day 5. The growth of untreated control U266 cells at day 1, day 3, and day 5 was 175%, 448%, and 972%, respectively.



therapeutic modalities has been attempted by many laboratories. One such approach is the chemotherapeutic intervention of the NF- κ B activation cascade (25, 32–34). In this study, we examined the effect of ACHP, a newly developed IKK inhibitor, on the growth of myeloma cells. We confirmed the previous observations of Bharti et al. (25, 35) that NF- κ B is constitutively activated in myeloma cells and found that ACHP could effectively inhibit the myeloma cell growth. We also found that the cell growth inhibitory effect of conventional antimyeloma compounds, vincristine and PAM, was significantly augmented when combined with ACHP. These findings support the idea that NF- κ B could be a feasible molecular target for the treatment of multiple myeloma.

Regarding the mechanism by which NF- κ B is activated in myeloma cells, we found the constitutive phosphorylation of p65 subunit of NF- κ B at Ser536 as well as that of I κ B α at Ser32. Although the constitutive phosphorylation of I κ B α at Ser32 has been reported in myeloma cells (25, 35), the constitutive phosphorylation of p65 has not been explored. There are at least three phosphorylation sites, Ser276, Ser529, and Ser536, within p65. Among these phosphorylation sites of p65, Ser536 phosphorylation plays crucial roles in the NF- κ B-mediated transactivation (36). For example, the point mutation of Ser536 eventually resulted in the lack of response to the lymphotoxin β receptor signaling (36) and the failure of nuclear translocation of NF- κ B (37). Owing to Ser536 being located within the carboxyl-terminal transactivation domain of p65, it is implicated in the transcriptional activity of NF- κ B once bound to the target DNA within the regulatory region of target genes by recruiting basal transcription factors and transcriptional coactivators (20, 36, 38). In contrast, although the Ser529 phosphorylation was found associated with the signal-induced NF- κ B activation through casein kinase II (39), it is unlikely that Ser529 plays a regulatory role in the NF- κ B activation cascade and its phosphorylation is considered to occur as a coincidence (40). Regarding the Ser276 phosphorylation of p65, both protein kinase A and mitogen- and stress-activated protein kinase 1 have been implicated and are considered to be involved in the NF- κ B activation by regulating the selective interaction with the p300/CREB-binding protein coactivator over histone deacetylase 1 (41, 42). However, other studies have shown that protein kinase A plays a negative role in the action of NF- κ B (43, 44). Thus, Ser536 phosphorylation plays a major role in the signal-mediated regulation of transcriptional competence of NF- κ B.

More importantly, the signal transduction pathways mediated by CD40L and B-cell activating factor have been shown to play important roles in the proliferation of myeloma cells. For example, B-cell activating factor is overexpressed in myeloma cells and involved in the protection from dexamethasone-induced apoptosis (45). In addition, CD40L is known to induce the proliferation and migration of myeloma cells by inducing NF- κ B through the activation of mitogen-activated protein kinases and phosphatidylinositol-3 kinase (5). In another report, it is shown that CD40/CD40L signaling activates NF- κ B by inducing the Ser536 phosphorylation of p65 (46). Although both IKK α and IKK β have been implicated in the Ser536 phosphorylation (36, 37, 40), the signaling cascades involving CD40L, B-cell activating factor, and lymphotoxin β require IKK α but not IKK β (36, 47, 48). Thus, IKK α could be a more feasible target for the treatment of multiple myeloma.

Furthermore, recent recognition of the noncanonical NF- κ B activation cascade, which is used by the signaling mediated by B-cell activating factor, CD40L, and lymphotoxin β , and primarily involving IKK α but not necessarily associated with phosphorylation of I κ B α proteins followed by their degradation, has highlighted the role of IKK α (49). Interestingly, the treatment of cells with a nuclear export inhibitor leptomycin B resulted in the nuclear accumulation of NF- κ B, I κ B α , NF- κ B-inducing kinase, and IKK α , but not IKK β , indicating that these proteins are shuttling between the cytoplasm and the nucleus even in the absence of any stimulation (50). Therefore, the sole inhibition of IKK β or proteasome may not be sufficient to suppress the NF- κ B activation associated with multiple myeloma.

In this study, ACHP exhibited the distinctive effective concentrations in inhibiting various features of myeloma cells. Although inhibition of the TNF α -mediated gene expression could occur at low ACHP concentration (<1 μ mol/L), higher concentrations (>10 μ mol/L) were required to inhibit the constitutive phosphorylation of p65, expression of NF- κ B-mediated genes, such as *cyclin D1*, *bcl-2*, *XIAP*, *c-IAP1*, and *IL-6*, and myeloma cell growth. These findings indicate that the growth inhibitory effect of ACHP may be through the inhibition of IKK α as well as IKK β .

In conclusion, our findings indicate the therapeutic efficacy of ACHP in inducing myeloma cell death presumably by blocking the constitutive activation of NF- κ B and the induction of antiapoptotic genes, thus sensitizing myeloma cells to cell death mediated by conventional antimyeloma agents. Although further efforts in drug development are necessary (i.e., the search for IKK α -specific compounds), our findings obtained with ACHP should give useful insights into a novel antimyeloma chemotherapy. Use of such compounds would conceivably reduce the dose of antimyeloma agents, prevent the side effects, enhance the adherence to chemotherapy, and augment the efficacy of the current myeloma chemotherapy.

ACKNOWLEDGMENTS

We thank Angelita Sarile for the language editing of this manuscript.

REFERENCES

1. Hideshima T, Anderson KC. Molecular mechanisms of novel therapeutic approaches for multiple myeloma. *Nat Rev Cancer* 2002;2:927–37.
2. Iida S, Ueda R. Multistep tumorigenesis of multiple myeloma: its molecular delineation. *Int J Hematol* 2003;77:207–12.
3. Dankbar B, Padro T, Leo R, et al. Vascular endothelial growth factor and interleukin-6 in paracrine tumor-stromal cell interactions in multiple myeloma. *Blood* 2000;95:2630–6.
4. Pahl HL. Activators and target genes of Rel/NF- κ B transcription factors. *Oncogene* 1999;18:6853–66.
5. Tai YT, Podar K, Mitsiades N, et al. CD40 induces human multiple myeloma cell migration via phosphatidylinositol 3-kinase/AKT/NF- κ B signaling. *Blood* 2003;101:2762–9.
6. Mitsiades CS, Mitsiades N, Poulaki V, et al. Activation of NF- κ B and up-regulation of intracellular antiapoptotic proteins via the IGF-1/Akt signaling in human multiple myeloma cells: therapeutic implications. *Oncogene* 2002;21:5673–83.
7. Hideshima T, Chauhan D, Schlossman R, Richardson P, Anderson KC. The role of tumor necrosis factor α in the pathophysiology of human multiple myeloma: therapeutic applications. *Oncogene* 2001;20:4519–27.

8. Mori N, Yamada Y, Ikeda S, et al. Bay 11-7082 inhibits transcription factor NF- κ B and induces apoptosis of HTLV-I-infected T-cell lines and primary adult T-cell leukemia cells. *Blood* 2002;100:1828-34.
9. Davis RE, Staudt LM. Molecular diagnosis of lymphoid malignancies by gene expression profiling. *Curr Opin Hematol* 2002;9:333-8.
10. Pikarsky E, Porat RM, Stein I, et al. NF- κ B functions as a tumour promoter in inflammation-associated cancer. *Nature* 2004;431:461-6.
11. Greten FR, Eckmann L, Greten TF, et al. IKK β links inflammation and tumorigenesis in a mouse model of colitis-associated cancer. *Cell* 2004;118:285-96.
12. Adams J. The proteasome: a suitable anticancer target. *Nat Rev Cancer* 2004;4:349-60.
13. Okamoto T, Sakurada S, Yang JP, Merin JP. Regulation of NF- κ B and disease control: identification of a novel serine kinase and thioredoxin as effectors for signal transduction pathway for NF- κ B activation. *Curr Top Cell Regul* 1997;35:149-61.
14. Nakano H, Shindo M, Sakon S, et al. Differential regulation of I κ B kinase α and β by two upstream kinases, NF- κ B-inducing kinase and mitogen-activated protein kinase/ERK kinase-1. *Proc Natl Acad Sci U S A* 1998;95:3537-42.
15. Yang J, Lin Y, Guo Z, et al. The essential role of MEKK3 in TNF-induced NF- κ B activation. *Nat Immunol* 2001;2:620-4.
16. DiDonato JA, Hayakawa M, Rothwarf DM, Zandi E, Karin M. A cytokine-responsive I κ B kinase that activates the transcription factor NF- κ B. *Nature* 1997;388:548-54.
17. Mercurio F, Zhu H, Murray BW, et al. IKK-1 and IKK-2: cytokine-activated I κ B kinases essential for NF- κ B activation. *Science* 1997;278:860-6.
18. Zandi E, Rothwarf DM, Delhase M, Hayakawa M, Karin M. The I κ B kinase complex (IKK) contains two kinase subunits, IKK α and IKK β , necessary for I κ B phosphorylation and NF- κ B activation. *Cell* 1997;91:243-52.
19. Sakurai H, Suzuki S, Kawasaki N, et al. Tumor necrosis factor- α -induced IKK phosphorylation of NF- κ B p65 on serine 536 is mediated through the TRAF2, TRAF5, and TAK1 signaling pathway. *J Biol Chem* 2003;278:36916-23.
20. Jiang X, Takahashi N, Ando K, et al. NF- κ B p65 transactivation domain is involved in the NF- κ B-inducing kinase pathway. *Biochem Biophys Res Commun* 2003;301:583-90.
21. Murata T, Shimada M, Sakakibara S, et al. Discovery of novel and selective IKK- β serine-threonine protein kinase inhibitors: Part I. *Bioorg Med Chem Lett* 2003;13:913-8.
22. Murata T, Shimada M, Sakakibara S, et al. Synthesis and structure-activity relationships of novel IKK- β inhibitors: Part 3. Orally active anti-inflammatory agents. *Bioorg Med Chem Lett* 2004;14:4019-22.
23. Kato M, Iida S, Komatsu H, Ueda R. Lack of ku80 alteration in multiple myeloma. *Jpn J Cancer Res* 2002;93:359-62.
24. Algarte M, Lecine P, Costello R, et al. *In vivo* regulation of interleukin-2 receptor α gene transcription by the coordinated binding of constitutive and inducible factors in human primary T cells. *EMBO J* 1995;14:5060-72.
25. Bharti AC, Donato N, Singh S, Aggarwal BB. Curcumin (diferuloylmethane) down-regulates the constitutive activation of nuclear factor- κ B and I κ B α kinase in human multiple myeloma cells, leading to suppression of proliferation and induction of apoptosis. *Blood* 2003;101:1053-62.
26. Yang JP, Hori M, Sanda T, Okamoto T. Identification of a novel inhibitor of nuclear factor- κ B, RelA-associated inhibitor. *J Biol Chem* 1999;274:15662-70.
27. Sato T, Asamitsu K, Yang JP, et al. Inhibition of human immunodeficiency virus type 1 replication by a bioavailable serine/threonine kinase inhibitor, fasudil hydrochloride. *AIDS Res Hum Retroviruses* 1998;14:293-8.
28. Ando T, Kawabe T, Ohara H, et al. Involvement of the interaction between p21 and proliferating cell nuclear antigen for the maintenance of G₂M arrest after DNA damage. *J Biol Chem* 2001;276:42971-7.
29. Kajino S, Suganuma M, Teranishi F, et al. Evidence that *de novo* protein synthesis is dispensable for antiapoptotic effects of NF- κ B. *Oncogene* 2000;19:2233-9.
30. Specht K, Haralambieva E, Bink K, et al. Different mechanisms of cyclin D1 overexpression in multiple myeloma revealed by fluorescence *in situ* hybridization and quantitative analysis of mRNA levels. *Blood* 2004.
31. Hideshima T, Bergsagel PL, Kuehl WM, Anderson KC. Advances in Biology of Multiple Myeloma: Clinical Applications. *Blood* 2004.
32. Hideshima T, Chauhan D, Richardson P, et al. NF- κ B as a therapeutic target in multiple myeloma. *J Biol Chem* 2002;277:16639-47.
33. Dai Y, Pei XY, Rahmani M, et al. Interruption of the NF- κ B pathway by Bay 11-7082 promotes UCN-01-mediated mitochondrial dysfunction and apoptosis in human multiple myeloma cells. *Blood* 2004;103:2761-70.
34. Mitsiades N, Mitsiades CS, Poulaki V, et al. Biologic sequelae of nuclear factor- κ B blockade in multiple myeloma: therapeutic applications. *Blood* 2002;99:4079-86.
35. Bharti AC, Shishodia S, Reuben JM, et al. Nuclear factor- κ B and STAT3 are constitutively active in CD138+ cells derived from multiple myeloma patients, and suppression of these transcription factors leads to apoptosis. *Blood* 2004;103:3175-84.
36. Jiang X, Takahashi N, Matsui N, Tetsuka T, Okamoto T. The NF- κ B activation in lymphotoxin β receptor signaling depends on the phosphorylation of p65 at serine 536. *J Biol Chem* 2003;278:919-26.
37. Mattioli I, Sebald A, Bucher C, et al. Transient and selective NF- κ B p65 serine 536 phosphorylation induced by T cell costimulation is mediated by I κ B kinase β and controls the kinetics of p65 Nuclear Import. *J Immunol* 2004;172:6336-44.
38. Asamitsu K, Tetsuka T, Kanazawa S, Okamoto T. RING finger protein AO7 supports NF- κ B-mediated transcription by interacting with the transactivation domain of the p65 subunit. *J Biol Chem* 2003;278:26879-87.
39. Wang D, Westerheide SD, Hanson JL, Baldwin AS Jr. Tumor necrosis factor α -induced phosphorylation of RelA/p65 on Ser529 is controlled by casein kinase II. *J Biol Chem* 2000;275:32592-7.
40. Sakurai H, Chiba H, Miyoshi H, Sugita T, Toriumi W. I κ B kinases phosphorylate NF- κ B p65 subunit on serine 536 in the transactivation domain. *J Biol Chem* 1999;274:30353-6.
41. Zhong H, May MJ, Jimi E, Ghosh S. The phosphorylation status of nuclear NF- κ B determines its association with CBP/p300 or HDAC-1. *Mol Cell* 2002;9:625-36.
42. Vermeulen L, De Wilde G, Van Damme P, Vanden Berghe W, Haegeman G. Transcriptional activation of the NF- κ B p65 subunit by mitogen- and stress-activated protein kinase-1 (MSK1). *EMBO J* 2003;22:1313-24.
43. Takahashi N, Tetsuka T, Uranishi H, Okamoto T. Inhibition of the NF- κ B transcriptional activity by protein kinase A. *Eur J Biochem* 2002;269:4559-65.
44. Neumann M, Grieshammer T, Chuvpilo S, et al. RelA/p65 is a molecular target for the immunosuppressive action of protein kinase A. *EMBO J* 1995;14:1991-2004.
45. Moreaux J, Legouffe E, Jourdan E, et al. BAFF and APRIL protect myeloma cells from apoptosis induced by interleukin 6 deprivation and dexamethasone. *Blood* 2004;103:3148-57.
46. Schwabe RF, Schnabl B, Kweon YO, Brenner DA. CD40 activates NF- κ B and c-Jun N-terminal kinase and enhances chemokine secretion on activated human hepatic stellate cells. *J Immunol* 2001;166:6812-9.
47. Coope HJ, Atkinson PG, Huhse B, et al. CD40 regulates the processing of NF- κ B2 p100 to p52. *EMBO J* 2002;21:5375-85.
48. Claudio E, Brown K, Park S, Wang H, Siebenlist U. BAFF-induced NEMO-independent processing of NF- κ B2 in maturing B cells. *Nat Immunol* 2002;3:958-65.
49. Pomerantz JL, Baltimore D. Two pathways to NF- κ B. *Mol Cell* 2002;10:693-5.
50. Birbach A, Gold P, Binder BR, et al. Signaling molecules of the NF- κ B pathway shuttle constitutively between cytoplasm and nucleus. *J Biol Chem* 2002;277:10842-51.

Q5
Q5

Positive correlation between sialyl Lewis X expression and pathological findings in renal cell carcinoma

Keiichi Tozawa, Takashi Okamoto, Noriyasu Kawai, Yoshihiro Hashimoto, Yutaro Hayashi,
Kenjiro Kohri

*From the Departments of Nephro-urology and Molecular Genetics, Nagoya City University,
Graduate School of Medical Sciences, 1 Kawasumi, Mizuho-cho, Mizuho-ku, Nagoya, Japan*

Corresponding author : Keiichi Tozawa

Address: 1 Kawasumi, Mizuho-cho, Mizuho-ku, Nagoya 467-8601, Japan

Telephone: +81-52-851-5511 (ext.8266)

Fax: +81-52-852-3179

E-mail: toza@med.nagoya-cu.ac.jp

Key words: sialyl Lewis antigen, renal cell carcinoma, cimetidin

Abstract

Background Interaction between tumor cells and endothelium plays a major role in cancer invasion and metastasis. Among various cell adhesion molecules, the cognate interaction between sialyl Lewis antigen expressed in the tumor cell surface and E-selectin expressed on endothelial cells are considered to be crucial for the tumor cell adhesion to the endothelium. **Methods** The sialyl Lewis X (sL^X) expression in 45 specimens from renal cell carcinoma (RCC) patients was examined using immunohistochemistry. **Results** In this study, we demonstrate that the immunoreactivity for sL^X in RCC specimens not only correlates with conventional histopathological parameters but also serves as a useful indicator for the prognosis of RCC. **Conclusions** Since beneficial effect of cimetidine has been reported and ascribed to its inhibitory action on the expression of E-selectin, a ligand molecule of sialyl Lewis antigen, cimetidine may also show inhibitory effect on the tumor recurrence and metastasis of RCC with high level of sLx expression.

Introduction

In order for tumor cells to metastasize, they first need to interact with endothelial cells. This cell-to-cell interaction requires the cognate interaction of cell adhesion molecules including E-selectin (tethering), and ICAM-1 and VCAM-1 (firm adhesion) that are expressed on the endothelial cell surface. Among these cell adhesion events the tethering step and thus the interaction between E-selectin and its ligand molecule sL antigens is considered crucial [1]. The ligands to E-selectin are sL antigens include sL X (sL^X) and sL A (sL^A). Recent reports have indicated that the beneficial effects of cimetidine for the patients with colorectal cancers are ascribed to its action in inhibiting E-selectin expression on the cell surface [2,3]. These experimental observations were confirmed by a randomized clinical trial of cimetidine, which clearly showed that the cimetidine treatment dramatically improved the survival of colorectal cancer patients with tumor cells expressing high levels of sL antigens but no such effects were found when sL expression levels were found low or null [3].

The sialyl Lewis antigen has been used as a useful marker for the diagnosis of various cancers in digestive organs, pancreas, gallbladder, liver, lung, and ovary [4-6]. The greater level of the sL^X expression was found in the metastasized lesions than the primary tumors in cases of bladder cancer [3]. Although the incidence and significance of expression of sL^X antigen in renal cell carcinoma (RCC) have ever been reported by only Cordon-Cardo et. al, cimetidine has been shown to have beneficial effects on the survival of patients with RCC [7]. In addition, Kinouchi et al. [8] reported that the combined therapy with interferon- α and cimetidine were effective even in advanced cases of RCC. Kobayashi et al. [9] found